DOI 10.2478/ama-2024-0053

NON-INVASIVE ANALYSIS OF THE BIOELECTRICAL IMPEDANCE OF A HUMAN FOREARM

Darius PLONIS*, Edas KALINAUSKAS, Andrius KATKEVIČIUS*, Audrius KRUKONIS***

*Vilnius Gediminas Technical University, Department of Electronic Systems, Vilnius, Lithuania,
**JSC Kongsberg NanoAvionics, Vilnius, Lithuania

darius.plonis@vilniustech.lt, edas.kalinauskas@nanoavionics.com, andrius.katkevicius@vilniustech.lt, audrius.krukonis@vilniustech.lt

received 02 April 2023, revised 16 October 2023, accepted 03 November 2023

Abstract: This study explores the practical application and impact of bioimpedance analysis in mobile devices for monitoring human health. The objective of the study is to propose a feasible application of non-invasive bioimpedance analysis by using the tetrapolar electrode connection method and the Cole–Cole model. Bioimpedance measurements and the calculation of electrical parameters are performed using ANSYS HFSS software for theoretical calculations and digital signal processing technology for real-time measurements using hardware devices. The study focuses on a model of the front arm, including tissues such as bone, fat, muscles, arteries and skin, with glucose concentrations as test cases. The simulated characteristic impedance with the ANSYS HFSS software package at 125 kHz varied from 315.8 Ω to 312.6 Ω, and the measured forearm characteristic impedance with hardware varied from 150.1 Ω to 151.3 Ω. The measured characteristic impedance when the heart is in systole and diastole also differed, with a difference of about 0.85% of the maximum impedance measured. The study demonstrates the potential of non-invasive bioimpedance analysis to address health issues such as obesity and heart disease. It also highlights its usefulness as a non-invasive alternative for measuring glucose concentration in diabetic patients to reduce the risk of infection. The findings indicate the feasibility of using bioimpedance analysis in mobile devices for health monitoring purposes.

Key words: non-invasive, bioimpedance, digital signal processing, human tissues

1. INTRODUCTION

Bioimpedance measurements are widely used in various fields [1–3]. Bioimpedance refers to the tissue's resistance to the flow of alternating electrical current. When an alternating electrical current passes through the human body, the Z complex impedance of the tissues consists of two components: the imaginary part (reactive resistance, X) and the real part (active resistance, R).

Bioimpedance measurement is based on the fact that the complex impedance of conductive materials depends on the shape of the conductor. In a cylindrical conductor, impedance is directly proportional to the length of the conductor and inversely proportional to the cross-sectional area of the conductor [4].

Different tissues in the body respond to electrical current such as conductors, semiconductors or dielectrics. Lean body tissues respond to electrical current as conductors because they contain a high amount of water and electrolytes. Fatty tissues and bones, on the other hand, act as dielectrics. Since electrical current will primarily flow through the most conductive tissues in the human body, such as interstitial fluids and muscles, these tissues will have the greatest influence on the overall body impedance.

Since the human body does not have a regular cylindrical shape, a model is used when measuring body impedance, in which different body parts are represented as separate cylindrical components: two arms, the human back and two legs [5].

When performing bioimpedance analysis and calculating body impedance, challenges arise because the human body consists of both active and reactive components of impedance. The reactive component of impedance in the human body is due to cell membranes, while the active component is influenced by intracellular and extracellular fluids. It can be inferred that cell membranes in the body act as capacitors, while intracellular and extracellular fluids function as resistors [6].

To calculate the reactive and active components of body impedance, several steps are involved. Firstly, the effective voltage and current values are calculated. Then, power and effective power are determined. Finally, phase shift, reactive impedance and active impedance can be calculated [7].

Currently, the most commonly used methods for electrode placement are bipolar and tetrapolar configurations. In bipolar electrode placement, two electrodes are connected to the human body to supply the tissue with alternating current and measure the voltage between the two electrodes. In tetrapolar electrode placement, four electrodes are used. Two electrodes are responsible for supplying the body with alternating current, while the other two measure the voltage [8].

When measuring the whole-body impedance, there are several methods for electrode placement on the body. These methods differ based on electrode attachment to different body locations, allowing the alternating current to flow through different segments of the human body. The most commonly used methods are hand-to-hand [9], foot-to-foot [10] and hand-to-foot [11] methods. Currently, the most popular method is the hand-to-foot method.

Segmental impedance analysis involves measuring the impedance of individual body segments. By measuring the impedance of specific body regions using this method, it is possible to

calculate the mass of different tissues in the entire body and monitor parameters such as heart activity, the relationship between impedance and blood glucose levels, and the respiratory rhythm of an individual [12,13].

In this method of measuring bioelectrical impedance, a constant frequency current of 50 kHz is commonly used. This current flows through electrodes attached to the individual's hand and foot [14]. By conducting measurements with a current of 50 kHz, it is possible to determine the fat-free mass and total body water content, but it is not possible to assess the specific quantities of intracellular and extracellular fluids since the 50 kHz current cannot penetrate cell membranes, which act as capacitors. Therefore, this method is most suitable for healthy individuals with a normal body water content and who are not severely dehydrated [15].

The limitations mentioned earlier can be overcome by the method of bioimpedance analysis using multiple frequency measurements, typically ranging from 0 kHz to 500 kHz (0, 1, 5, 50, 100, 200 and 500). This method is based on the principle that different tissues have different electrical conductivities at different frequencies. By applying currents at different frequencies, it is possible to estimate fat-free mass, total body water and the quantities of extracellular and intracellular fluids. Research has shown that using variable-frequency electrical currents allows for more accurate estimation of extracellular fluids [16]. However, a previous study [17] has indicated that this method is not suitable for determining the distribution of water between intracellular and extracellular compartments in the bodies of elderly individuals.

Another application area is in the measurement of fat-free mass. The initial methods for calculating fat-free mass were solely based on measurements of height and impedance. To improve measurement accuracy, formulas were later derived that required additional individual data such as weight, age, sex, reactance and anthropometric [18]. In this method, a constant current of 50 kHz, 800 μA is used to calculate bioimpedance. Kotler et al. [19] developed a formula specifically for calculating fat-free mass in healthy individuals. This method utilises a fixed-frequency 50 kHz electrical current for impedance measurement.

In the human body, body fluids consist of intracellular (ICW) and extracellular (ECW) fluids. Studies have shown that bioelectrical impedance analysis at varying frequencies is more suitable for measuring body fluids as it yields lower measurement errors [20].

This method involves measuring impedance at varying frequencies. A current with frequencies ranging from 0 kHz to 100 kHz was passed through the human body. Impedance was measured at specific frequencies: 1 kHz, 5 kHz, 50 kHz and 100 kHz. The results showed that the most accurate determination of the total body fluid volume was obtained using an electrical current of 100 kHz, while the most accurate data for extracellular fluid volume were obtained using an electrical current of 1 kHz. Kushner and Schoeller [21] derived a formula for calculating the total body fluid volume.

Constant frequency bioelectrical impedance analysis is also used to determine the total body skeletal muscle mass [22].

Equally important research has been conducted in a previous study [23], stating that under different pressures in the arteries, their diameter can vary from 2.274 mm to 2.519 mm. Another study [24] presents an electrical model of arterial impedance variation due to the heart pulse. It is also crucial to note that blood conductivity and dielectric permittivity parameters vary with changes in blood glucose levels. In a study by Li et al. [25], the calculation was made on how glucose affects the electrical parameters of deionised water at glucose concentrations ranging from 0 mmol/L to 225 mmol/L.

In addition, in this study, it was observed that dielectric permittivity parameters, conductivity and dielectric relaxation time have a linear dependence on the glucose concentration in deionised water solution. Based on this finding, formulas were derived to calculate the electrical parameters of the solution at different glucose concentrations [22]. The observation that glucose affects the conductivity of a non-conductive solution leads to the conclusion that different glucose concentrations also affect the electrical conductivity of blood. Therefore, by knowing the electrical parameters of blood, the diameter and length of the artery at the measurement site, it is possible to calculate bioimpedance [26].

To measure bioimpedance, a tetrapolar 4-electrode connection method was used. This method was chosen because the shape of electrodes, and contact impedance has less influence on measurement accuracy than the bipolar measurement method. In the tetrapolar configuration, a current is applied through two electrodes, while the other two electrodes are used for voltage measurement. No current flows through the voltage measurement electrodes. The entire electrical current passes only through the tested tissue. Consequently, there is no voltage drop due to contact impedance between the voltage measurement electrodes. Additionally, when performing measurements using the tetrapolar connection method, the body position has less impact than the bipolar measurement method. Finally, the tetrapolar electrode configuration method is less sensitive to electrode placement than the bipolar method.

This study will be conducted on the human wrist. This location was chosen because it is convenient to measure the variation in bioimpedance due to the presence of the radial and ulnar arteries in the wrist. The radial and ulnar arteries are among the main arteries in the human body.

2. INVESTIGATED MODELS OF THE FOREARM

The described study consists of two parts: theoretical and experimental. In the theoretical part, computer modelling of bioimpedance analysis is performed using the ANSYS HFSS software package. In the experimental part, bioimpedance measurements are taken on the human wrist using a specially prepared measurement setup.

2.1. Computer-based model of the forearm using ANSYS HFSS

The electrical model of the forearm was created using the ANSYS HFSS software package, considering six tissues: the skin layer, adipose tissue, arteries, muscles, cortical bone and bone marrow (Fig. 1).

The length of the electrical spatial model is 25 cm, the width is 5.05 cm and the height is 3.05 cm. The proportions and thickness of the selected tissues in the study were the same as those used in the study conducted by Yu et al. [1] Dimensions of the model are provided in Fig. 2. In the model (Fig. 1), the skin layer is depicted in orange, adipose tissue in yellow, arteries in red, muscles in pink, cortical bone in grey and bone marrow in white. Green colour represents the electrodes used to connect to the tissues.

DOI 10.2478/ama-2024-0053

The electrodes located on the outer surface of the model are current electrodes, while the electrodes at the centre are voltage electrodes. During the development of the model, separate parameters were defined, allowing for easy modification of the length, width, height, artery diameter and electrode layout of the model. In the centre of the model, a space was created to visualise the distribution of current within the model.

The power source for bioelectrical impedance measurements in the ANSYS HFSS software package was implemented using current sources. The amplitude of the current was chosen to be 0.1 mA. The selected maximum current value is safe and complies with the IEC 60601-2-47:2012 safety standard for medical electrical equipment – Part 2-47: Particular requirements for the basic safety and essential performance of ambulatory electrocardiographic systems. This choice was made in consideration of the capabilities of the experimental equipment that will be used in subsequent experiments.

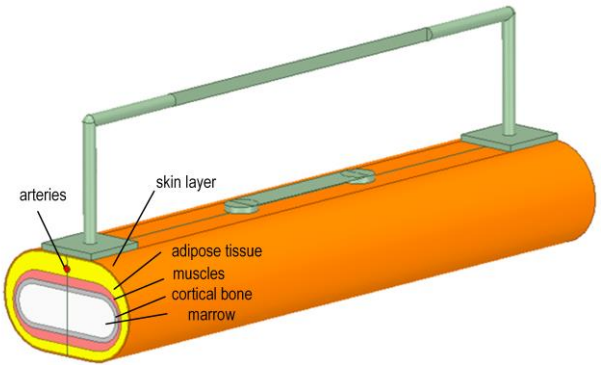

Fig. 1. Computer model of the human forearm, created using the ANSYS HFSS software package, consists of the following components: the skin layer in orange, adipose tissue in yellow, arteries in red, muscles in pink, cortical bone in grey and bone marrow in white

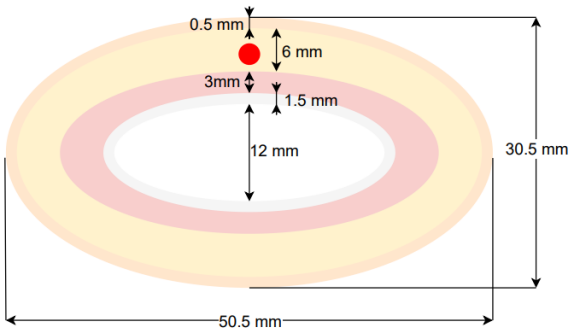

Fig. 2. Dimensions of the tissues in the model

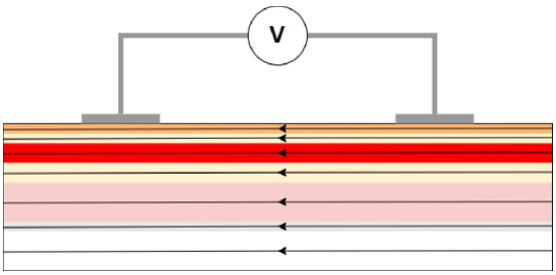

Fig. 3. Distribution of current through the tissues in the forearm electrical model [15]

The ANSYS HFSS software package cannot automatically calculate the bioelectrical impedance using current sources. Therefore, it needs to be calculated using the field calculator function. To do this, firstly, the voltage drop between the voltage measurement electrodes needs to be calculated. This can be done by knowing the electric field and the distance between two points.

The voltage drop was calculated using the field calculator tool in the ANSYS HFSS software package. The expression of Ohm's law was used to calculate the bioelectrical impedance.

The current flow in each tissue depends on the geometry and electrical parameters of the tissues. Since the geometry of the tissues in the thigh is irregular and complex, it is challenging to create an accurate electrical model. For this reason, the model will be composed of stacked tissues. The forearm model is shown in Fig. 3.

By creating such a model, it can be concluded that the current distributes through all the tissues of the forearm. Since the tissues in the model are connected in parallel, this model is equivalent to an electrical model of six resistors connected in parallel, and their total resistance can be calculated using formula [15]:

$$\frac{1}{Z_{fa}} = \frac{1}{Z_{bm}} + \frac{1}{Z_{cb}} + \frac{1}{Z_m} + \frac{1}{Z_f} + \frac{1}{Z_b} + \frac{1}{Z_s}, \quad (1)$$

where Z_{fa} is the characteristic impedance of the forearm, Z_{bm} is the characteristic impedance of the bone marrow, Z_{cb} is the characteristic impedance of cortical bone, Z_m is the characteristic impedance of muscle, Z_f is the characteristic impedance of fat, Z_b is the characteristic impedance of blood and Z_s is the characteristic impedance of the skin.

To calculate the resistance of an individual tissue, the tissue's electrical conductivity needs to be known. With this value, the tissue resistance can be calculated using formula [15]:

$$R_{tiss} = \frac{l}{\sigma_{tiss} \cdot A_{tiss}}, \quad (2)$$

where R_{tiss} is the resistance of the tissue, L is the distance, σ_{tiss} is the electrical conductivity of the tissue and A_{tiss} is the cross-sectional area of the tissue.

During the computer modelling of the human wrist, three parameters were varied: frequency, radial artery diameter and different glucose concentrations in the blood. The radial artery diameter of the human wrist was limited to two different values ranging from 2.274 mm to 2.519 mm. Four different glucose concentrations in the blood were used to calculate the characteristic resistances of the simulated human wrist model in ANSYS HFSS software. In total, calculations were performed at 48 different frequency points. The calculated results of the model are presented on a logarithmic frequency scale to visualise the variation in the characteristic resistances, especially at lower frequencies.

2.2. Physical forearm measurement model

Bioelectrical impedance was measured using the MAX30001 integrated circuit. The MAX30001 circuit is a complete solution for wearable applications and serves as a biopotential and bioimpedance front analogue. It provides high performance and extremely low power consumption to extend battery life in clinical and fitness applications. In a single biopotential channel, it provides a form of pulse in the electrocardiogram (ECG), heart rate and pacemaker edge detection. In addition, there is a single bioimpedance channel to measure breathing.

sciendo
DOI 10.2478/ama-2024-0053

The bioimpedance channel is equipped with integrated programmable current drives that support common electrodes and provide flexibility for measuring two or four electrodes.

During the measurements, the maximum allowable frequency of MAX3001 was used, which is 128 kHz. A 1 kHz high-frequency filter was applied to the voltage measurement electrode inputs. This filter is designed to eliminate high-frequency noise from bioelectrical impedance measurements. Two MAX3001 integrated operational amplifiers were used during the measurements. The first operational amplifier was set to operate in a low-noise mode. The gain coefficient of the second operational amplifier was set to 20 V/V. The analogue-to-digital converter sampling frequency was set to the maximum possible value of 64 Hz. The integrated digital filters of the MAX3001 prototype were not used since all signal processing will be performed using the MATLAB software package. The amplitude of the alternating electrical current was set to the maximum allowable value of 0.096 mA.

The real physical experiment setup, using the MAX3001 prototype with four electrodes, is shown in Fig. 4. The four electrodes were arranged equidistantly on the human forearm. Real physical experiments were conducted on a healthy individual without diabetes. The glucose concentration in the blood was measured using a commercial glucometer – CONTOUR PLUS ELITE.

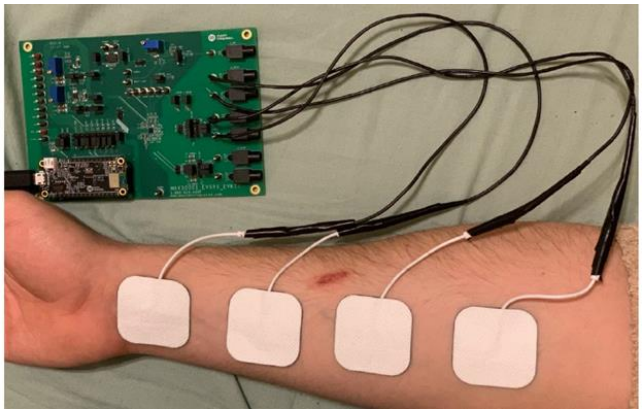

Fig. 4. Physical measurements of the characteristic impedance based on the MAX30001 integrated circuit

The MAX30001 integrated circuit is connected to an external microcontroller, which is used to collect and process information. Samples are recorded in 20-bit resolution. This sensor calculates the characteristic impedance based on the following formula [6]:

$$Z(\Omega) = ADC \cdot \frac{V_{ref}}{2^{19} \cdot CG_{MAG} \cdot GAIN}, \quad (4)$$

where ADC is the voltage reading from the analogue-to-digital converter of the sensor, V_{ref} is the reference voltage, CG_{MAG} is the magnitude of the current excitation and $GAIN$ is the internal gain applied to the voltage measurement.

This integrated circuit was chosen for its small size, low cost and ease of operation. Due to these characteristics, this sensor is suitable for use not only in scientific research but also in commercial products.

The tested individual should fasting for 8 h. The person was tested when in a lying position, fully relaxed. Initially, the blood glucose level was measured before glucose consumption. After measuring the blood glucose concentration, the subject consumed 75 g of glucose. The next measurement was taken 30 min after glucose intake, and subsequent measurements were taken every 30 min. The test lasted a total of 90 min. A total of four measurements of glucose and characteristic impedance were taken. Each measurement of characteristic impedance lasted 5 min to capture multiple readings of impedance changes and increase the reliability of the test. The testing equipment and its setup are shown in Fig. 4.

After conducting the measurements of characteristic impedance, the previously discussed signal processing was performed to remove noise caused by human respiration and electrical interference.

3. SIGNAL PROCESSING METHODS

The planned measurements are expected to be quite noisy, so it is important to discuss possible signal processing methods. The most common sources of noise include human movements, respiration and electrical interference. The initial unprocessed measurement results with evident low-frequency noise influenced by human respiration are presented in Fig. 5. Fig. 5 shows a 30 s data window with characteristic impedance calculations from raw data.

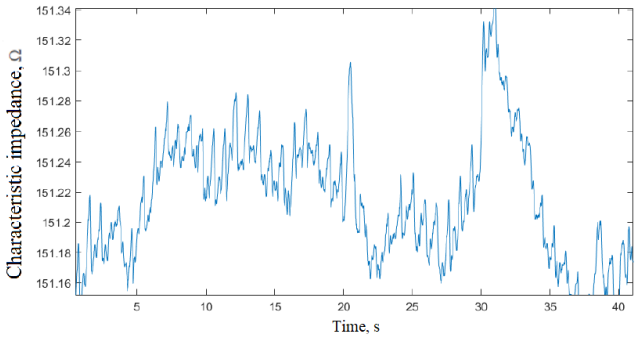

Fig. 5. Example of characteristic impedance calculated from raw data

The aforementioned filtering helps to eliminate the previously mentioned sources of noise, such as respiration and electrical interference. From the filtered signal, peak values of the signal can be extracted. Each signal maximum and minimum indicate the impedance during systole and diastole of the heart, respectively (Fig. 6).

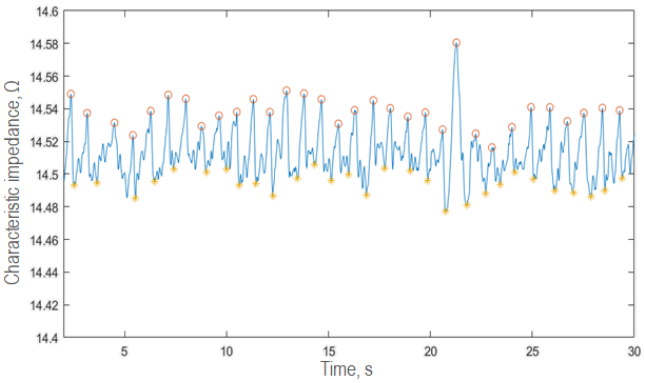

Fig. 6. Calculated characteristic impedance from raw data with the applied Chebyshev bandpass filter

DOI 10.2478/ama-2024-0053

A hundredth-order Chebyshev bandpass filter was designed for the initial data filtering by using the MATLAB software package. The sampling frequency was chosen to be 130 Hz, justified by the hardware used. The MAX3001 sampling rate was 64 Hz. The passband of the bandpass filter was set from 0.7 Hz to 40 Hz. Frequencies below 0.7 Hz were filtered out to eliminate the influence of respiration on the measurements [27]. The heart rate in the human body ranges from 50 beats/min to 180 beats/min, corresponding to frequencies from 0.8 Hz to 3 Hz. This filter ensures that such heart rate frequencies are captured. The upper cutoff frequency of the passband was chosen to be 40 Hz to filter out electrical interference present in the measurements. The filter has a stopband attenuation of 80 dB at the filtered frequencies.

4. RESULTS

In this section, computer modelling results using the ANSYS HFSS software package and experimental research results under real conditions are presented to validate the hardware on the human wrist.

4.1. Characteristic impedance results of computer-based modelling

Computer modelling using the ANSYS HFSS software package yielded results of the wrist computer model's characteristic impedance dependence on the frequency and blood glucose level. Computer modelling was performed in the frequency range from 10 kHz to 2 MHz. During the experiments, the blood glucose level was varied within the range of 4 mmol/L to 33 mmol/L.

The results of the variation in the characteristic impedance when the blood glucose concentration is 4 mmol/L are shown in Fig. 7. The graph displays three curves. The orange curve represents the characteristic impedance when the heart is in the systolic state. The blue curve represents the characteristic impedance when the heart is in the diastolic state. The grey curve shows the difference in the characteristic impedance between different heart states as a function of frequency. The initial analysis of the results indicates that the model's characteristic impedance is inversely proportional to the frequency of the alternating current.

As the artery fills with blood during systole, the pressure and diameter of the artery increase. At this moment, there is more electrically conductive blood in the artery, resulting in a lower value of characteristic impedance than the diastolic state when there is less blood in the artery and the diameter is reduced. The characteristic impedance during systole, as the frequency increases, varies from 330.86 Ω to 229.13 Ω in our examined frequency range from 10 KHz till 2 MHz. During diastole, the characteristic impedance varies from 332.99 Ω to 229.53 Ω.

The difference between the characteristic impedances is not directly dependent on the frequency of the alternating current. As shown in Fig. 8, initially, there is an increasing difference at lower frequencies. The difference reaches its maximum at around 150 kHz and then starts to decrease again. Throughout the frequency range, the difference varies from 0.39 Ω to 2.13 Ω. It can be concluded that at 150 kHz, the difference between the characteristic impedance of blood and the overall model impedance is the greatest, indicating the highest concentration of current in the artery. The current distribution in the other layers of the model is minimal. Since the highest current concentration is in the artery at 150 kHz, the largest difference between the characteristic impedances is observed when the heart is in systole and diastole. As the frequency increases, the characteristic impedance of the other model tissues decreases faster than the blood impedance, resulting in a smaller variation in characteristic impedance for the different cardiac states.

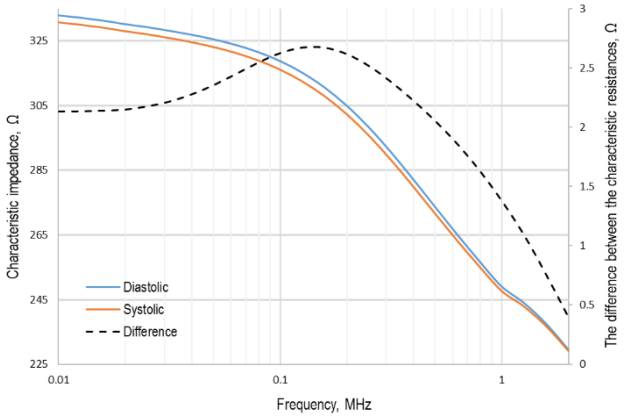

Fig. 7. Change in characteristic impedance with respect to the artery diameter and frequency, when the glucose concentration in the blood is 4 mmol/l

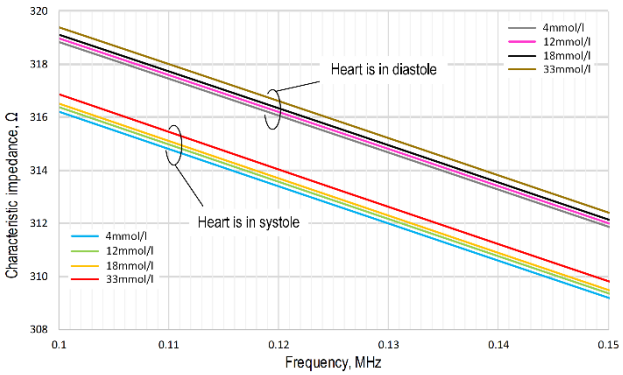

Fig. 8. Change in characteristic impedance as the artery diameter, frequency and glucose concentration vary

Since the overall model impedance is more dependent on frequency than on blood glucose concentration to better visualise the dependence of the characteristic impedance on glucose concentration and frequency, the results are presented in a narrower frequency range from 100 kHz to 150 kHz. This dependence is shown in Fig. 8. In Fig. 8, two groups of curves can be distinguished. The red, orange, green and blue curves represent the results of the characteristic impedance when the heart is in systole, while the brown, black, pink and grey curves represent the results when the heart is in diastole. In systole, the blood glucose concentrations were chosen as follows: red – 33 mmol/l, orange – 18 mmol/l, green – 12 mmol/l and blue – 4 mmol/l. In diastole, the blood glucose concentrations were chosen as follows: brown – 33 mmol/l, black – 18 mmol/l, pink – 12 mmol/l and grey – 4 mmol/l. As seen in the graph, different blood glucose concentrations lead to changes in the overall model's characteristic impedance. With varying glucose concentrations and different cardiac states (systole and diastole), the characteristic impedance varies throughout the frequency range. Thus, the blood glucose concentration is directly proportional to the characteristic impedance of the entire model of the human wrist current.

To investigate the dependence of the difference between the characteristic impedance of the heart in systole and diastole on glucose concentration, the values of characteristic impedance were examined at 125 kHz. This frequency was chosen because it is the closest frequency that our used hardware is capable of measuring, and it is close to the frequency of 150 kHz, where the largest difference between the characteristic impedance of the wrist in systole and diastole is observed. This dependence is shown in Fig. 9.

From the graph, it can be observed that the difference in the characteristic impedance of the whole model is inversely proportional to the glucose concentration in the blood. When the glucose concentration is 4 mmol/l, the difference in characteristic impedance is 2.674 Ω. When the glucose concentration is 12 mmol/l, the difference between the characteristic impedances in the model, in systole and diastole, is 2.645 Ω. When the glucose concentration is 18 mmol/l, the difference in impedances is 2.636 Ω. When the glucose concentration is 33 mmol/l, the difference in impedances is 2.578 Ω. These calculated results confirm the previous assumption that the difference in characteristic impedances between systole and diastole decreases with increasing glucose concentration in the blood.

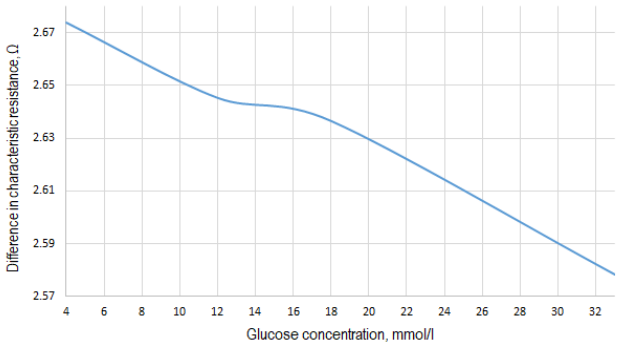

Fig. 9. Dependence of the difference between the characteristic impedance of the wrist in systole and diastole on glucose concentration, when the frequency is 125 kHz

4.2. Characteristic impedance results of the physical experiment

The equipment for measuring the characteristic impedance and the procedure of measurements and the entire experimental study are described in the previous section. For each 5-min measurement, the values of the characteristic impedance in systole were subtracted from the values in diastole. The average difference was then calculated. The measured glucose concentration values and the average values of the impedance differences are presented in Fig. 10.

The blue curve (Fig. 10) represents the measured glucose concentration using the commercial glucometer CONTOUR PLUS ELITE. The orange curve represents the measured difference in characteristic impedance between systole and diastole. From the graph in Fig. 11, it can be observed that as the glucose concentration in the blood increases, the difference in characteristic impedance decreases. Conversely, as the glucose concentration decreases, the difference in characteristic impedance increases. At the initial time, the measured glucose concentration was 4.5 mmol/l, and the difference in characteristic impedance was 67 mΩ. After 30 min of consuming 75 g of glucose, the glucose concentration in the blood increased to 8.1 mmol/l, and the difference in characteristic impedance at that time was 43.4 mΩ. After 60 min from the start of the test, the glucose concentration in the blood decreased to 6.2 mmol/l, and the average difference in characteristic impedance increased to 60.7 mΩ. At the final time, after 90 min from glucose consumption, the glucose concentration in the blood dropped to 4.8 mmol/l, and the difference in characteristic impedance increased to 64.4 mΩ. The measured values of the difference in characteristic impedance and glucose concentration are presented in Tab. 1.

From the conducted test, it is evident that the difference in characteristic impedance between systole and diastole has an opposite relationship to the difference in characteristic impedance. The dependence of the difference in characteristic impedance on glucose is depicted in Fig. 11.

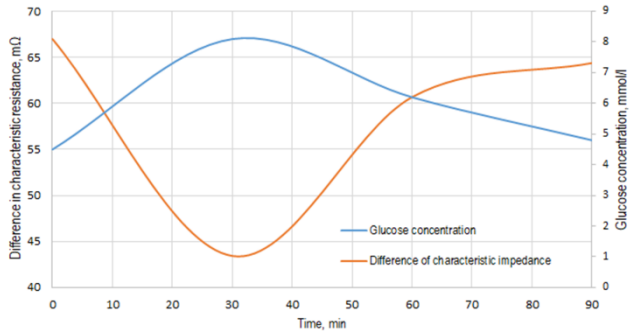

Fig. 10. Measurement of glucose concentration in the blood and difference in bioelectric impedance

Tab. 1. Values of measured glucose concentration in blood and the differences in characteristic impedance in systolic and diastolic states

Time (min)	Glucose concentration (mmol/l)	Differences in characteristic impedance (mΩ)
0	4.5	67
30	8.1	43.4
60	6.2	60.7
90	4.8	64.4

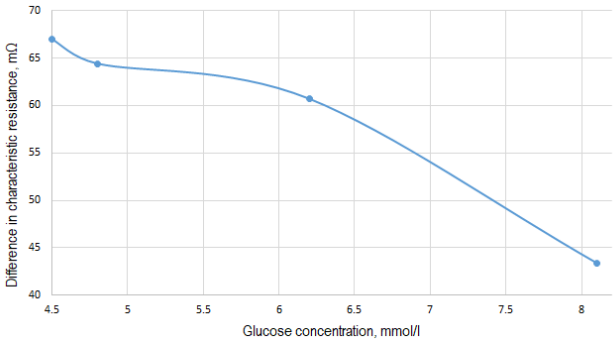

Fig. 11. Dependencies of the differences in the characteristic impedance when the heart is in systolic and diastolic states on blood glucose concentration

The (Fig. 11) shows that the relationship between the difference in characteristic impedance and glucose concentration is not linear. Due to this nonlinearity, it may be challenging to accurately

DOI 10.2478/ama-2024-0053

calculate the exact glucose concentration in the blood based on the measurement of the difference in characteristic impedance between systole and diastole.

5. DISCUSSION

In the study, the characteristic impedance of the entire forearm was measured under real conditions and by creating a forearm computer model and measuring its impedance using the ANSYS HFSS software package. Despite using the same electrode size and arrangement in both the software package and the real measurements, a significant difference in characteristic impedance was observed. Through calculations with the software package, the characteristic impedance of the entire forearm varied from 315.8 Ω to 312.6 Ω at a frequency of 125 kHz, depending on the different states of the heart and different glucose concentrations in the blood. When measuring the characteristic impedance under real conditions, the impedance of the entire forearm ranged from 150.1 Ω to 151.3 Ω due to low-frequency noise caused by respiration and different glucose concentrations in the blood, as well as different states of the cardiac cycle.

As can be seen, the measurements differ significantly. This difference arises because not all tissues present in the human forearm were included in the model. The forearm contains tissues that are more conductive to electrical current than fat, bone and skin. Due to the presence of these more conductive tissues, the actual characteristic impedance of the entire forearm is lower than what was calculated using the software package. Tissues such as tendons, arterial walls, extracellular fluids and other tissues were not represented in the model.

The measurements also differ because the proportions of muscle, fat, artery, bone and skin tissues vary between the measured individual and the model. In reality, the individual may have more blood vessels, which are more conductive to electrical current, than what was included in the designed model. Additionally, the forearm not only contains the radial artery but also the ulnar artery, which is smaller in size but still a good conductor of electricity.

When performing calculations with the ANSYS HFSS software package, it was observed that the model's characteristic impedance varied significantly when the heart was in the systolic and diastolic states, with a maximum change occurring at a blood glucose concentration of 4 mmol/l. At this glucose concentration, the model's characteristic impedance ranged from 312.57 Ω to 315.25 Ω. The difference between these two impedances was 2.67 Ω, corresponding to a 0.85% variation from the maximum characteristic impedance value.

During real measurements using the MAX30001 hardware, it was observed that the characteristic impedance varied, on average, by about 67 mΩ at a glucose concentration of 4.5 mmol/l. The average measured characteristic impedance over a 5-min period was 151.21 mΩ at a glucose concentration of 4.5 mmol/l. This variation in characteristic impedance corresponds to a 0.04% change from the average measured characteristic impedance.

When measuring the results under real conditions, much smaller variations in characteristic impedance were obtained than those in the calculations using ANSYS HFSS software. Although the variations in characteristic impedance due to the heart rate differ significantly, both the theoretical calculations and the actual measurements showed the same dependency of characteristic impedance on the heart rate. The significant discrepancy between the results obtained in the software and the measurements under real conditions could be attributed to the fact that not all tissues present in the forearm were included in the model. Tissues such as tendons, arterial walls, extracellular fluids and veins were not included in the model. These tissues are more conductive to electrical current than skin, fat or bones, but their characteristic impedance does not depend on the heart rate. Therefore, in real conditions, the electrical current distributes through more electrically conductive tissues, and the variation in characteristic impedance of the radial artery has a smaller impact on the overall characteristic impedance of the forearm.

The results obtained from the calculations using ANSYS HFSS software showed that the variation in the model's characteristic impedance, when the heart is in systole and diastole, is inversely proportional to the glucose concentration in the blood. When the measurement frequency of the characteristic impedance was set to 125 kHz, and the glucose concentration was 4 mmol/l, the variation in the characteristic impedance due to the heartbeat was 2.67 Ω. When the glucose concentration reached 12 mmol/l, the variation in the characteristic impedance was 2.65 Ω. For a glucose concentration of 18 mmol/l, the impedance variation was 2.64 Ω. When the glucose concentration reached its highest level of 33 mmol/l, the impedance variation was 2.58 Ω.

During the measurements under real conditions, although the measured glucose concentrations differed from the concentrations used in software, the same dependence of the characteristic impedance variation was observed as in the calculations with software. When the measured glucose concentration was 4.5 mmol/l, the variation in the characteristic impedance was 0.067 mΩ. At a glucose concentration of 4.8 mmol/l, the measured variation in the characteristic impedance due to the heartbeat was 64.6 mΩ. With an increase in glucose concentration to 6.2 mmol/l, the variation in the characteristic impedance was 60.7 mΩ, and when the maximum glucose level of 8.1 mmol/l was reached, the variation in the characteristic impedance was 64.4 mΩ.

6. CONCLUSIONS

After conducting a literature review on the characteristic impedance of the human body, the electrical model of the human body was analysed. The main parameters of the body's characteristic impedance were reviewed, and an overview of different measurement methods for the characteristic impedance was conducted.

In the scope of this study, a computer model of the human wrist was developed using the ANSYS HFSS software package. Additionally, measurements of the bioelectrical characteristic impedance were performed with different glucose concentrations in the blood. The characteristic impedance of the wrist was also measured using the MAX30001 integrated circuit at various glucose concentrations in the blood, and the measured characteristic impedance signals were processed programmatically.

The measurements using the ANSYS HFSS software package revealed that the characteristic impedance of the wrist is inversely proportional to the glucose concentration in the blood. Using the software package, the characteristic impedance of the wrist was also calculated when the heart is in systole and diastole, resulting in changes in the diameter of the radial artery in the wrist. The difference in characteristic impedance between the maximum and minimum diameter of the radial artery was calculated, and the dependence of this difference on the glucose con-

centration in the blood was examined. The results showed that the difference in characteristic impedance is inversely dependent on the glucose concentration in the blood.

The measurements conducted using the MAX30001 integrated circuit confirmed the results obtained from the computer simulation. The largest difference in impedance between systole and diastole was observed at 150 kHz. By performing calculations with different glucose concentrations in the blood, it was observed that the difference in characteristic impedance is inversely proportional to the glucose concentration in the blood. All measurements were performed in the frequency range from 10 kHz to 2 MHz. The glucose concentration in the model artery varied from 4 mmol/l to 33 mmol/l.

The measured values of the model and real wrist's characteristic impedance revealed a significant difference, which arose due to the absence of all tissues in the computer model created with ANSYS HFSS. In future work, there are plans to improve the computer model of the human wrist by including as many tissues as possible that are actually present in the human wrist.

The study conducted using ANSYS HFSS software showed that the wrist's characteristic impedance is inversely proportional to the frequency of the alternating current, and the model's characteristic impedance is higher when the heart is in the diastolic state.

In this feasibility study on non-invasive bioelectric impedance analysis, we recognised that changes in physical parameters of the human hand can lead to changes in measurements. However, since the main objective of the study was to determine the technical effectiveness of the method, a complete study of these variations was not part of the scope. Recognising the importance of individual differences in hand anatomy, we believe that in the future, more comprehensive research will take these parameters into account to ensure robust and accurate application of non-invasive biomechanical analysis.

REFERENCES

1. Yu Y, Anand G, Lowe A, Zhang H, Kalra A. Towards estimating arterial diameter using bioimpedance spectroscopy: a computational simulation and tissue phantom analysis. Sensors 2022;22(13):4736. https://doi.org/10.3390/s22134736
2. Jacob J, Ishaan B, Onyezili F. Diabetes induction with streptozotocin and insulin action on blood glucose levels in albino rats. International Journal of Modern Science and Technology. 2021;3(10):208–212.
3. Eyth E, Basit H, Swift CJ. Glucose tolerance test. StatPearls [Internet] 2023 Apr [cited 2023 Jul 18]. Available from: https://www.ncbi.nlm.nih.gov/books/NBK532915/
4. Kushner RF. Bioelectrical Impedance Analysis: A Review of Principles and Applications. The American Journal of Clinical Nutrition. 1992;11(2):199-209. https://doi.org/10.1080/07315724.1992.12098245
5. Patterson R. Body Fluid Determinations Using Multiple Impedance Measurements. IEEE Engineering in Medicine and Biology Magazine. 1989;8(1):16–18. https://doi.org/10.1109/51.32399
6. Anamika P, Mukesh R. Bioimpedance analysis of vascular tissue and fluid flow in human and plant body: A review. Biosystems Engineering. 2020; 197: 170–187. https://doi.org/10.1016/j.biosystemseng.2020.06.006
7. Cpindean R, Holonec R, Dragan F, Muresan C. Method for Body Impedance Measuremen. 6th International Conference on Advancements of Medicine and Health Care through Technology. 2018:17–20. Cluj-Napoca, Romania. IFMBE Proceedings 71. Springer, Singapore. https://doi.org/10.1007/978-981-13-6207-1_13
8. Critcher S, Freeborn TJ. Multi-Site Impedance Measurement System based on MAX30001 Integrated-Circuit. 2020 IEEE 63rd International Midwest Symposium on Circuits and Systems (MWSCAS). Springfield, MA, USA. 2020:381–386. https://doi.org/10.1109/MWSCAS48704.2020.9184451
9. Ghosh S, Meister D, Cowen S, Hannan JW, Ferguson A. Body composition at the bedside. Eur. J. Gastroenterol. Hepatol. 1997; 9(8): 783–788. https://doi.org/10.1097/00042737-199708000-00009
10. Nuñez C, Gallagher D, Visser M, Pi-Sunyer FX, Wang Z, Heymsfield SB. Bioimpedance analysis: Evaluation of leg-to-leg system based on pressure contact footpad electrodes. Med Sci Sports Exerc. 1997; 29(4):524–531. https://doi.org/10.1097/00005768-199704000-00015
11. Hoffer EC, Meador CK, Simpson DC. Correlation of whole-body impedance with total body water volume. J. Appl. Physiol. 1969; 27(4):531–534. https://doi.org/10.1152/jappl.1969.27.4.531
12. Bera TK. Bioelectrical Impedance Methods for Noninvasive Health Monitoring: A Review, Journal of medical engineering. 2014:381251. https://doi.org/10.1155/2014/381251
13. Moonen HPFX, Van Zanten ARH. Bioelectric impedance analysis for body composition measurement and other potential clinical applications in critical illness. Current Opinion in Critical Care. 2021 27(4):344–353. https://doi.org/10.1097/MCC.0000000000000840
14. Utter AC, Nieman DC, Ward AN, Butterworth DE. Use of the leg-to-leg bioelectrical impedance method in assessing body-composition change in obese women. The American Journal of Clinical Nutrition. 1999;69(4):603–607. https://doi.org/10.1093/ajcn/69.4.603
15. Heymsfield SB, Nuñez C, Testolin C, Gallagher D. Anthropometry and methods of body composition measurement for research and field application in the elderly. European Journal of Clinical Nutrition. 2000;54(3):526–532. https://doi.org/10.1038/sj.ejcn.1601022
16. Patel RV, Peterson EL, Silverman N, Zarowitz BJ. Estimation of total body and extracellular water in post-coronary artery bypass surgical patients using single and multiple frequency bioimpedance. Critical Care Medicine Journal. 1996;24(11):1824–1828. https://doi.org/10.1097/00003246-199611000-00011
17. Olde Rikkert MG, Deurenberg P, Jansen RW, Van't Hof MA, Hoefnagels WH. Validation of multifrequency bioelectrical impedance analysis in detecting changes in geriatric patients. Journal of the American Geriatrics Society. 1997;45(11):1345–1351. https://doi.org/10.1111/j.1532-5415.1997.tb02934.x
18. Kyle UG, Genton L, Karsegard L, Slosman DO, Pichard C. Single prediction equation for bioelectrical impedance analysis in adults aged 20–94 years. Nutrition. 2001;17(3):248–253. https://doi.org/10.1016/s0899-9007(00)00553-0
19. Kotler DP, Burastero S, Wang J, Pierson RNJr. Prediction of body cell mass, fat-free mass, and total body water with bioelectrical impedance analysis: effects of race, sex, and disease. The American Journal of Clinical Nutrition. 1996;64(3):489–497. https://doi.org/10.1093/ajcn/64.3.489s
20. Deurenberg P, Tagliabue A, Schouten FJ. Multi-frequency impedance for the prediction of extracellular water and total body water. British Journal of Nutrition. 1995;73(3):349–358. https://doi.org/10.1079/bjn19950038
21. Kushner RF, Schoeller DA. Estimation of total body water by bioelectrical impedance analysis. The American Journal of Clinical Nutrition. 1986;44(3):417–424. https://doi.org/10.1093/ajcn/44.3.417
22. Kyle UG, Bosaeus I, De Lorenzo AD, Deurenberg P, Elia M, Gómez JM, Heitmann BL, Kent-Smith L, Melchior JC, Pirlich M, Scharfetter H, Schols AM, Pichard C. Composition of the ESPEN Working Group. Bioelectrical impedance analysis--part I: review of principles and methods. Clinical Nutrition. 2004;23(5):1226–1243. https://doi.org/10.1016/j.clnu.2004.06.004
23. Chamiot-Clerc P, Copie X, Renaud JF, Safar M, Girerd X. Comparative reactivity and mechanical properties of human isolated internal mammary and radial arteries. Cardiovascular Research. 1998;37(3): 811–819. https://doi.org/10.1016/S0008-6363(97)00267-8

DOI 10.2478/ama-2024-0053

24. Cho MC, Kim JY, Cho SH. A bio-impedance measurement system for portable monitoring of heart rate and pulse wave velocity using small body area, 2009 IEEE International Symposium on Circuits and Systems (ISCAS). 2009;3106–3109. http://dx.doi.org/10.1109/ISCAS.2009.5118460
25. Li J, Igbe T, Liu Y, Nie Z, Qin W, Wang L, Hao Y. An approach for noninvasive blood glucose monitoring based on bioimpedance difference considering blood volume pulsation. IEEE Access. 2018;6: 51119–51129. https://doi.org/10.1109/ACCESS.2018.2866601
26. Karacolak T, Moreland RC, Topsakal R. Cole-Cole model for glucose-dependent dielectric properties of blood plasma for continuous glucose monitoring. Microwave and Optical Technology Letters. 2013;55(5):1160–1164. https://doi.org/10.1002/mop.27515
27. Bailon R, Sornmo L, Laguna P. ECG derived respiratory frequency estimation. Advanced Methods and Tools for ECG Data Analysis. 2006; 215–243.

Darius Plonis: https://orcid.org/0000-0001-6579-1526
Edas Kalinauskas: https://orcid.org/0009-0006-1608-4749
Andrius Katkevičius: https://orcid.org/0000-0002-1623-5643
Audrius Krukonis: https://orcid.org/0000-0002-4694-781X